Experimental demonstration of voltage-gated spin-orbit torque switching in an antiferromagnet/ferromagnet structure

Weixiang Li,[1,2,3] Shouzhong Peng,[1,2,*] Jiaqi Lu,[1,2,3] Hao Wu,[4] Xiang Li,[4] Danrong Xiong,[1] Yan Zhang,[3] Youguang Zhang,[3] Kang L. Wang,[4] and Weisheng Zhao[1,2,†]

[1]*Fert Beijing Institute, MIIT Key Laboratory of Spintronics, School of Integrated Circuit Science and Engineering, Beihang University, Beijing 100191, China*

[2]*Hefei Innovation Research Institute, Beihang University, Hefei 230013, China*

[3]*School of Electronic and Information Engineering, Beihang University, Beijing 100191, China*

[4]*Department of Electrical Engineering, University of California, Los Angeles, Los Angeles, California 90095, USA*

(Received 23 July 2020; revised 4 March 2021; accepted 5 March 2021; published 23 March 2021)

Efficient manipulation of magnetization is crucial for magnetic random-access memory (MRAM). Here we experimentally demonstrate spin-orbit-torque-driven (SOT-driven) magnetization switching of perpendicularly magnetized IrMn/CoFeB/MgO structures with the assist of a gate voltage. It is found that with the gate voltage changing from −0.6 to 0.6 V, the SOT critical switching current density J_c is reduced by 59%. Furthermore, the mechanism of voltage-induced J_c reduction is explored. We find that the dampinglike torque decreases with positive voltage, while the fieldlike torque shows a weak voltage dependence, which demonstrates that the voltage control of spin-orbit torque (VCSOT) effect has no positive effect on the reduction of J_c. In addition, a significant decrease of anisotropy energy is observed when a positive voltage is applied. These results indicate that both VCSOT effect and voltage control of magnetic anisotropy (VCMA) effect exist in voltage-gated SOT switching, while the VCMA effect plays a main role in reduction of J_c. This work shows low-power magnetization switching and helps to understand the mechanism of voltage-gated SOT switching.

DOI: 10.1103/PhysRevB.103.094436

I. INTRODUCTION

Magnetic random-access memory (MRAM) is a great candidate for next-generation memory devices due to its nonvolatility, high speed, low power consumption, and high density [1–5]. How to achieve energy-efficient magnetization switching is one of the main challenges for MRAM. Spin transfer torque (STT) shows its superiority because it is driven by current, which makes STT-MRAM simple to integrate with existing complementary metal-oxide semiconductor (CMOS) circuits [6–8]. But common read/write paths make STT-MRAM suffer from read disturbances and barrier breakdown limitations. Spin-orbit torque (SOT), in which the write path is separated from the read path, has gained great attention in attempts to overcome read disturbances problems [9–12]. In addition, SOT has the advantages of high write speed and low risk of breakdown. However, an external in-plane field is usually required to break symmetry for deterministic switching of perpendicular magnetization. The antiferromagnet/ferromagnet (AFM/FM) system is proposed to achieve field-free SOT switching, in which case an in-plane exchange bias field induced by exchange coupling can replace the external magnetic field [13–19].

Nevertheless, a large current is usually needed for the SOT-driven magnetization switching of the AFM/FM structure due to the small in-plane exchange bias and the low spin Hall angle [13]. Therefore, it is critical to reduce the SOT critical switching current to achieve low power consumption. One of the promising methods for low-power switching is the combination of SOT with a gate voltage. By applying a gate voltage at the top electrode, the critical current density J_c can be reduced, but its mechanism is not clear. One possible mechanism is voltage control of the spin-orbit torque (VCSOT) effect. Some groups found that a gate voltage could be used to control spin-orbit field by changing the magnitude of the interfacial spin-orbit interaction [20,21]. Thus the SOT critical current density J_c may be reduced by enhancing the spin-orbit fields with a gate voltage. Furthermore, the voltage control of magnetic anisotropy (VCMA) effect is another way, because a gate voltage may lower the perpendicular magnetic anisotropy (PMA) [20,22–29]. The mechanism of the VCMA effect is regarded as the voltage-induced charge accumulation or depletion and change of orbital hybridizations at the ferromagnet/oxide interface [30], which lowers the interfacial PMA and the energy barrier. Therefore the gate voltage may be used to assist SOT switching because of the VCMA effect.

Yoda *et al.* and Inokuchi *et al.* succeeded in achieving magnetization switching of magnetic tunnel junctions (MJTs) with in-plane magnetic anisotropy by voltage-gated SOT [31,32]. The former used voltage as a selecting principle and SOT effect as a writing principle, and the latter improved read disturb and write error rates by adjusting the timing relation of write current and gate voltage. Both of them attribute this phenomenon to the VCMA effect. However, Chen *et al.* found

*shouzhong.peng@buaa.edu.cn
†weisheng.zhao@buaa.edu.cn

 ©2021 American Physical Society

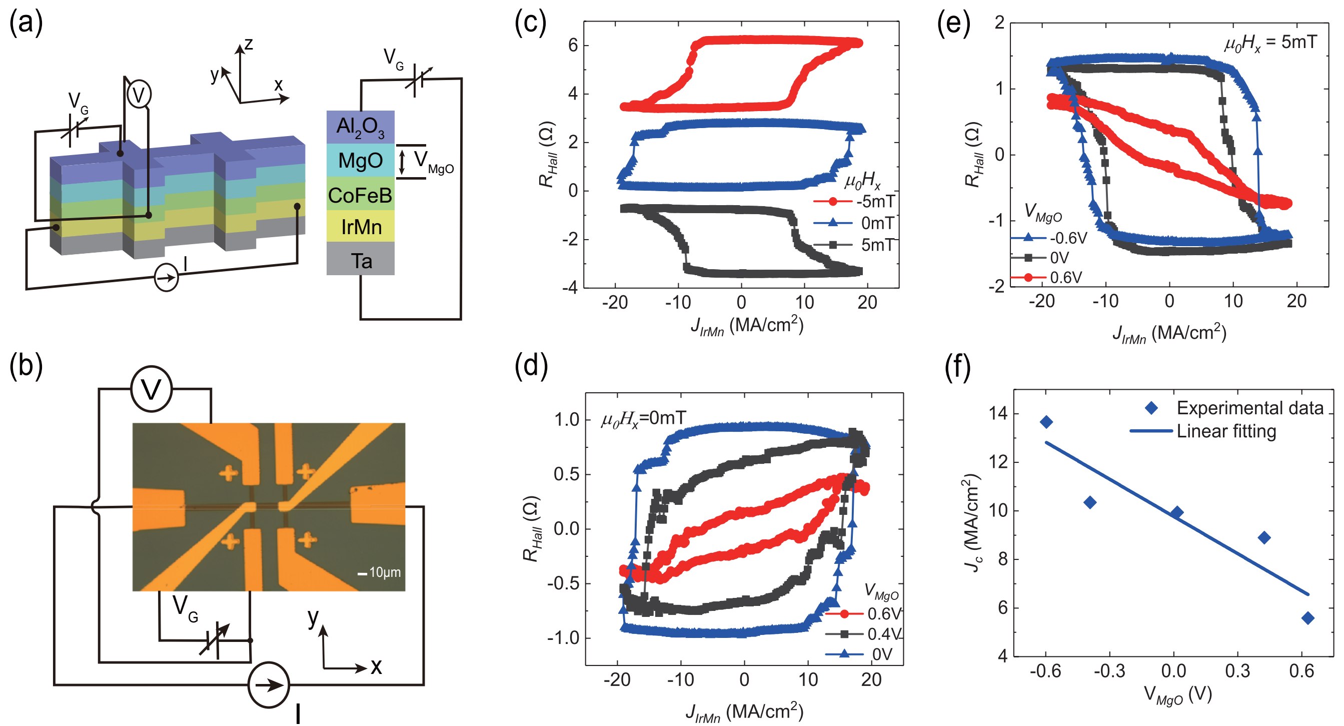

FIG. 1. (a) Schematic of IrMn/CoFeB/MgO structures. (b) Micrograph of the Hall bar and measurement setup. (c) SOT-driven magnetization switching with various in-plane external fields. Voltage-gated SOT switching under different gate voltages with (d) no external field and (e) 5-mT in-plane external field. (f) Critical current density J_c dependence on voltage applied to MgO (V_{MgO}) with 5-mT field applied.

that the VCMA effect may not be the only source in voltage-gated SOT switching, because the change in critical current I_c is much greater than that in the magnetic anisotropy field H_k [20]. Therefore it is necessary to explore the mechanism of voltage-gated SOT switching, especially in perpendicularly magnetized AFM/FM systems.

In this paper we demonstrate field-free SOT switching and investigate the voltage-gated SOT switching in the perpendicularly magnetized IrMn/CoFeB/MgO structures. To clarify the mechanism of voltage-gated SOT switching, the effective torques including dampinglike and fieldlike torques under various voltages are characterized using the harmonic technique. Furthermore, to explore the VCMA effect, the interfacial anisotropy K_i under different control voltages is calculated from the in-plane hysteresis loop. We demonstrate that both the VCSOT effect and VCMA effect exist in voltage-gated SOT switching. However, the VCSOT effect has no positive effect on the reduction of J_c, because the dampinglike torque decreases with a positive voltage applied. Meanwhile, the VCMA effect brings about a significant decrease of anisotropy energy, which contributes to the J_c reduction.

II. DEVICE FABRICATION AND VOLTAGE-GATED SOT SWITCHING

The film structures used in this study are Ta (2 nm)/IrMn (5 nm)/CoFeB (1.34 nm)/MgO (2.5 nm)/Al_2O_3(5 nm) deposited on thermally oxidized Si substrate by magnetron sputtering as shown in Fig. 1(a). The film is annealed at 200 °C for 30 min under vacuum with 1.5-T in-plane external field along the x direction to obtain strong perpendicular magnetic anisotropy (PMA) and in-plane exchange bias, and then the sample is patterned into a Hall bar with 5 μm width current channel and 3 μm width voltage channel grown by standard ion beam etching (IBE) and lithography. The film is covered with a 33-nm-thick Al_2O_3 layer with atomic layer deposition to diminish leakage current. Figure 1(b) shows the micrograph of the Hall bar and the measurement setup. The saturation magnetization (M_S) is measured to be 1157 kA/m. All the measurements are performed at room temperature.

In the following we perform the SOT-driven magnetization switching. An incremental in-plane pulse current of 10-ms pulse width flows along the x direction, and meanwhile the Hall resistance is measured. In the middle of each pulse is a 100-ms delay time. The Hall resistance changes with the current pulse increasing, and the results are shown in Fig. 1(c). There is a clear clockwise switching loop under a 5-mT longitudinal external field and a reverse direction switching loop under the −5-mT field, which is a noteworthy feature in SOT-driven magnetization switching [33,34]. Field-free switching is achieved when the loop is in the same direction as the switching loop under a −5-mT field, which means exchange bias is in the negative direction. Furthermore, to explore voltage-gated SOT switching, a gate voltage is applied at the top electrode, and the switching loops are obtained with no external field applied, as shown in Fig. 1(d). The critical current density J_c is defined as the value of pulse current when R_{Hall} changes over half. J_c is obviously reduced by applying a positive voltage; however, it needs larger current to switch the magnetization under negative voltage, which breaks down the sample. Thus we investigate the voltage-gated SOT-driven magnetization switching with 5 mT applied field. During

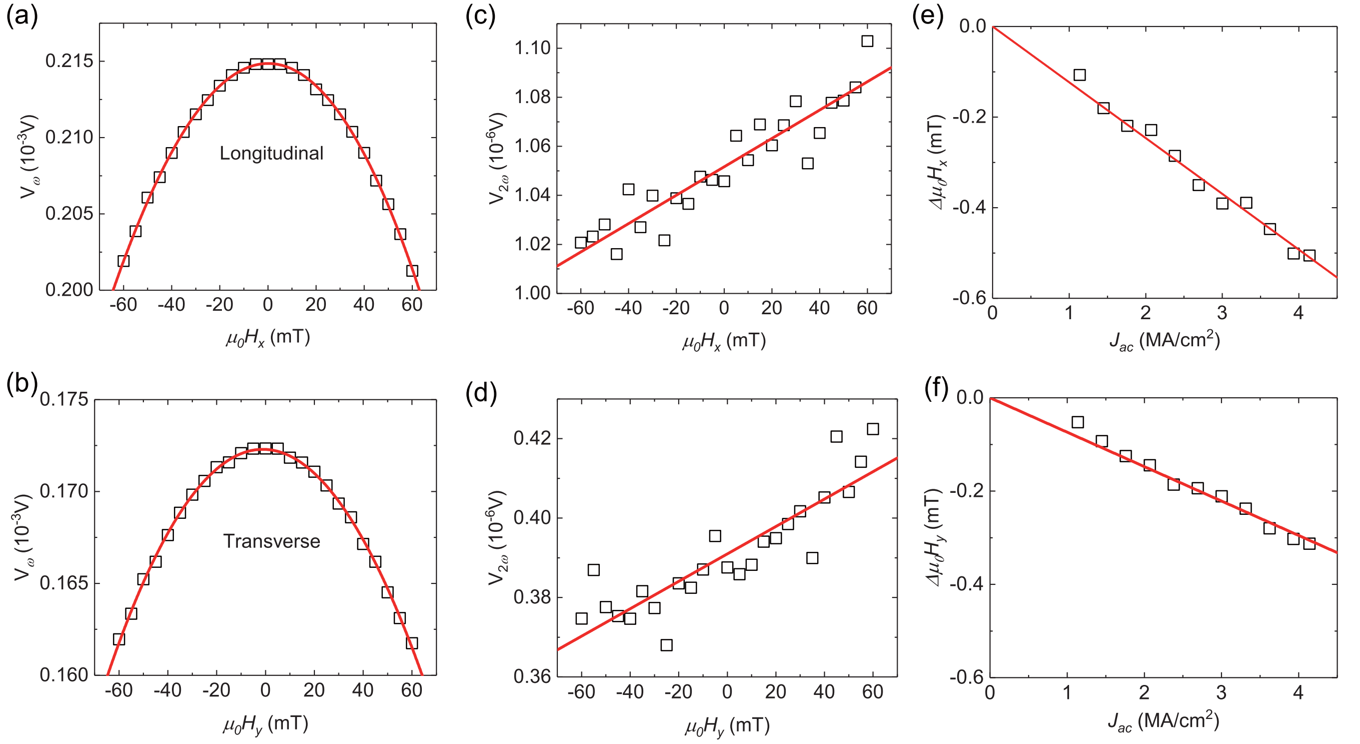

FIG. 2. (a), (b) First and (c), (d) second harmonic signals for (a), (c) longitudinal and (b), (d) transverse measurements with $J_{ac} = 2.07\,\mathrm{MA/cm^2}$ under gate voltage of 0 V. (e) Dampinglike torque and (f) fieldlike torque dependence of current density extracted by fitting the first and second harmonic signal.

measurements, when a gate voltage of 15 V is applied on the top electrode, the voltage in the MgO layer (V_{MgO}) is about 0.6 V. In particular, the leakage current has no impact on voltage-gated SOT-driven magnetization switching (see Supplemental Material S1 [35]). Figure 1(f) presents critical current densities with a 5-mT field under different gate voltages. Critical current density J_c ($13.7\,\mathrm{MA/cm^2}$) under a V_{MgO} of -0.6 V is about 2.5 times larger than that ($5.6\,\mathrm{MA/cm^2}$) under V_{MgO} of 0.6 V. The critical current density J_c shows a decreasing tendency with increasing V_{MgO}. These results indicate that a gate voltage can be used to effectively modulate SOT-driven perpendicular magnetization switching, and this is a feasible writing method for low energy consumption.

III. VOLTAGE CONTROL OF THE SPIN-ORBIT TORQUE EFFECT

To explore voltage control of spin-orbit torque (VCSOT) effect, we quantify the magnitude of spin-orbit torques, including dampinglike and fieldlike torques using the harmonic technique [34,36,37], with different gate voltages. A small sinusoidal current (frequency 133.33 Hz) is applied to generate harmonic signals, and meanwhile the harmonic Hall voltage signals are measured with lock-in amplifiers. We sweep the external field along the in-plane (x and y) direction to obtain the longitudinal and transverse components of the effective field. The magnetic field $\mu_0H_{x(y)}$ is slightly tilted off-plane to prevent domain nucleation and ensure the magnetic moment is switched by the external field. Figure 2 shows the dependence of harmonic signals on the in-plane external field with an ac current peak of 1 mA ($2.07\,\mathrm{MA/cm^2}$) under a gate voltage of 0 V (set the voltage source to 0 V). Figures 2(a) and 2(b) show the first harmonic signal V_ω with the external field sweeping along the longitudinal and transverse direction. The first signal V_ω scales with the square of magnetization field, and the quadratic coefficients $\partial^2V_\omega/\partial H_{x(y)}^2$ are extracted by optimal fitting. Figures 2(c) and 2(d) show the second harmonic signal $V_{2\omega}$ when the external field sweeps along the longitudinal and transverse directions. $V_{2\omega}$ is linearly dependent on field, and the slope $\partial V_{2\omega}/\partial H_{x(y)}$ is extracted from linear fitting. Respectively, the dampinglike torque $\Delta\mu_0H_x$ and the fieldlike torque $\Delta\mu_0H_y$ are obtained from Eq. (1) [34], and they show a linear relation with current density, as shown in Figs. 2(e) and 2(f):

$$\Delta\mu_0H_{x(y)} = -2\frac{\partial V_{2\omega}}{\partial H_{x(y)}}\Bigg/\frac{\partial^2V_\omega}{\partial {H_{x(y)}}^2}. \tag{1}$$

We choose the slope of optimal fitting of $\mu_0H_{x(y)} - J_{ac}$ to represent their strength. Figure 3 presents the effective magnetic field dependence on voltage in the MgO layer V_{MgO}. The dampinglike torque efficiency decreases with positive voltage increasing, whereas the fieldlike torque efficiency shows weaker voltage dependence. These results demonstrate that V_{MgO} can modulate spin torques in the IrMn/CoFeB/MgO system. Due to the short screening length of the CoFeB layer, the voltage at the IrMn/CoFeB interface is much smaller than that at the CoFeB/MgO interface. The VCSOT effect is expected to mainly originate from the change of spin torques at the CoFeB/MgO interface rather than that at the IrMn/CoFeB interface. Figure 3 shows the total spin torques at

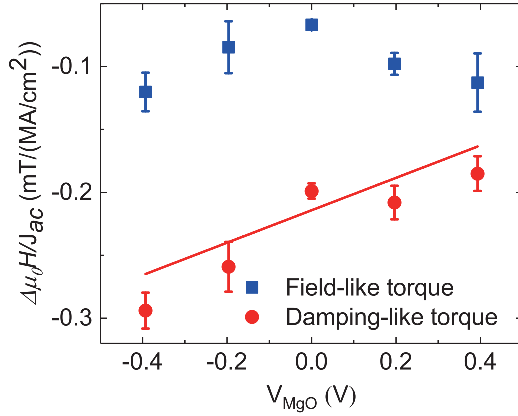

FIG. 3. The dependence of $\Delta\mu_0 H_x/J_{ac}$ and $\Delta\mu_0 H_y/J_{ac}$ on voltage in MgO layer (V_{MgO}). The error bars are standard deviations.

the CoFeB/MgO interface and IrMn/CoFeB interface [20,21]. The dampinglike torque efficiency under V_{MgO} of -0.4 V is 1.5 times larger than that under V_{MgO} of 0.4 V, while the field-like torque efficiency changes little with voltage. The fieldlike torque is considered to make magnetization of CoFeB rotating about easy axis and it does not affect R_{Hall}. The decrease of dampinglike torque efficiency leads to the decrease of θ_{SHE} [34], which means a larger J_c is required for the magnetization switching under positive voltage. Through the VCSOT effect, positive voltage tends to increase J_c, which is opposite the experimental results in Fig. 1(f). Therefore the VCSOT effect is not the reason for the reduction of J_c in the voltage-gated SOT switching, and there are other effects in voltage-gated SOT-driven magnetization switching.

IV. VOLTAGE CONTROL OF MAGNETIC ANISOTROPY EFFECT

Next we discuss quantitatively the effect of voltage on perpendicular magnetic anisotropy. In-plane hysteresis loops at different gate voltages are obtained as shown in Fig. 4(a). The Hall resistance is measured by scanning the longitudinal external field along the x direction with a small direct current (100 μA). When a positive magnetic field is applied, R_{Hall} decreases with positive voltage, which indicates the reduction of PMA. The anisotropy energy K_{eff} (V_{MgO}) and the interfacial anisotropy constant $K_i(V_{\text{MgO}})$ under different V_{MgO} is obtained from Eq. (2) [38] and Eq. (3) [38], respectively:

$$K_{\text{eff}}(V_{\text{MgO}}) = \mu_0 M_S \int_0^1 H_x d\left(\frac{M_x}{M_S}\right), \tag{2}$$

$$K_i(V_{\text{MgO}}) = \left[K_{\text{eff}}(V_{\text{MgO}}) + \frac{1}{2}\mu_0 M_S^2\right] \times t_{\text{CoFeB}}. \tag{3}$$

Specifically, in an in-plane hysteresis loop,

$$\left(\frac{M_x}{M_S}\right) = \sqrt{1-(M_z/M_S)^2} = \sqrt{2\left(\frac{R_{\text{Hall}}-R_{\text{Hall}}^{\text{Min}}}{R_{\text{Hall}}^{\text{Max}}-R_{\text{Hall}}^{\text{Min}}}\right)^2-1}\,. \tag{4}$$

Here μ_0 is the permeability of free space, M_S is the saturation magnetization, which is measured to be 1157 KA/m, H_x is the x component of the external field, $M_x(M_z)$ is the x component (z component) of magnetization, R_{Hall} is the

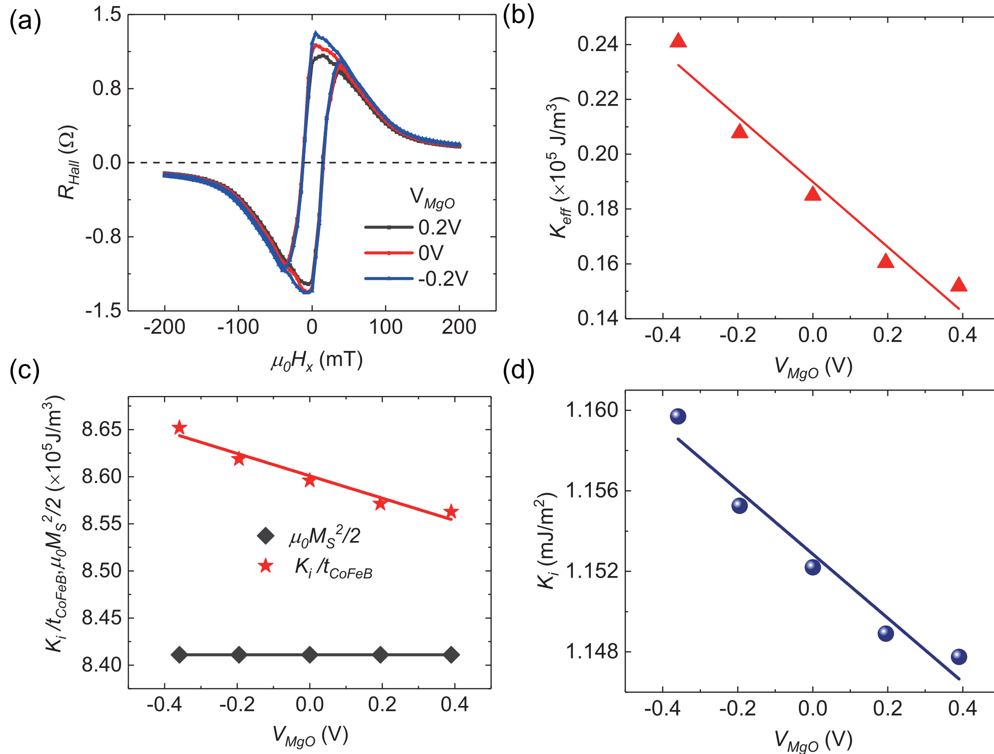

FIG. 4. (a) Anomalous Hall resistance (R_{Hall}) under different gate voltages (V_{MgO}). (b) K_{eff}, (c) K_i/t_{CoFeB} and $\mu_0 M_S^2/2$, and (d) K_i dependence on V_{MgO}.

anomalous Hall resistance, and $R_{\mathrm{Hall}}^{\mathrm{Min}}$ ($R_{\mathrm{Hall}}^{\mathrm{Max}}$) is the minimum (maximum) value of R_{Hall}. The exact value $R_{\mathrm{Hall}}^{\mathrm{Min}}$ ($R_{\mathrm{Hall}}^{\mathrm{Max}}$) is obtain from perpendicular magnetization hysteresis loops. t is the thickness of the free layer, which is 1.34 nm.

The dependence of anisotropy energy $K_{\mathrm{eff}}(V_{\mathrm{MgO}})$ on gate voltage is shown in Fig. 4(b). According to Ref. [39], J_c is proportional to $(\frac{H_{K,\mathrm{eff}}}{2} - \frac{H_x}{\sqrt{2}})$:

$$J_C = \frac{2e}{\hbar}\frac{\mu_0 M_S t}{\theta_{SHE}}\left(\frac{H_{K,\mathrm{eff}}}{2} - \frac{H_x}{\sqrt{2}}\right), \tag{5}$$

where $H_{K,\mathrm{eff}}$ is the effective anisotropy field, e is the elementary charge, and $\hbar$ is the reduced Planck constant. As shown in Fig. 4(b), K_{eff} decreases by 37% when V_{MgO} changes from -0.4 to 0.4 V, which leads to a decrease of $\frac{H_{K,\mathrm{eff}}}{2} - \frac{H_x}{\sqrt{2}}$ by 45%. At the same time, the dampinglike torque decreases by 37% (see Fig. 3). Therefore the critical current density J_c will decrease by 13% when V_{MgO} varies from -0.4 to 0.4 V, in line with Eq. (5). As demonstrated in Fig. 1(f), J_c decreases by 14% in our experiments, which is consistent with the calculated result (13%) from Eq. (5). More details can be found in the Supplemental Material S2 [35]. In addition, the critical current J_c decreases as the anisotropy energy K_{eff} increases, which can be found in the Supplemental Material S3 [35]. These results clearly show that the decrease of J_c in the voltage-gate SOT switching is mainly caused by the reduction of PMA due to the VCMA effect.

Furthermore, the K_i/t_{CoFeB} and $\mu_0 M_S^2/2$ are obtained from Eqs. (2) and (3), as shown in Fig. 4(c). The value of K_i/t_{CoFeB} varies linearly with V_{MgO} while $\mu_0 M_S^2/2$ is a constant (see Supplemental Material S4 [35]). Figure 4(d) shows the interfacial anisotropy coefficient K_i. We can see that the K_i changes linearly with V_{MgO} due to the VCMA effect. From the slope of the linear fitting, the VCMA coefficient ξ of 34.3 fJ/Vm is obtained for the IrMn/CoFeB/MgO structure. Through comparison of Figs. 4(b) and 4(c) we can see that K_i/t_{CoFeB} is one order of magnitude lager than K_{eff}. By subtracting $\mu_0 M_S^2/2$, a small variation of K_i contributes to a significant change of K_{eff}, which results in a significant change of PMA.

V. CONCLUSION

In summary, this work demonstrated voltage-gated SOT switching in IrMn/CoFeB/MgO structures and shed light on the underlying mechanism. The critical current J_c was reduced by 59% when the V_{MgO} was changed from -0.6 to 0.6 V. Dampinglike and fieldlike torques under different gate voltages were measured to clarify the mechanism of voltage-gated SOT switching. We found that dampinglike torque decreases with increasing positive voltage, while fieldlike torque shows a weak voltage dependence. In addition, the changes of K_i and K_{eff} under different gate voltages were obtained from an in-plane hysteresis loop. A small variation of K_i led to a significant change of K_{eff}, which brought about the reduction of J_c. These results demonstrated that both the VCSOT effect and VCMA effect exist in voltage-gated SOT switching. But the VCSOT effect hindered the reduction of J_c, while the VCMA effect made a main contribution to the J_c reduction. This work provides a comprehensive understanding of voltage-gated SOT switching and shows the potential to achieve low-power data writing with the voltage-gated SOT method.

ACKNOWLEDGMENTS

The authors thank the National Natural Science Foundation of China (Grants No. 62004013, No. 61627813, and No. 61571023), the International Collaboration Project (No. B16001), the National Key Technology Program of China (Contract No. 2017ZX01032101), and the Beihang Hefei Innovation Research Institute (Project No. BHKX-19-02) for their financial support of this work.

[1] S. Bhatti, R. Sbiaa, A. Hirohata, H. Ohno, S. Fukami, and S. N. Piramanayagam, Mater. Today **20**, 530 (2017).
[2] K.W. Kim, K. J. Lee, H. W. Lee, and M. D. Stiles, Phys. Rev. B **94**, 184402 (2016).
[3] M. Wang, W. Cai, K. Cao, J. Zhou, J. Wrona, S. Peng, H. Yang, J. Wei, W. Kang, Y. Zhang, J. Langer, B. Ocker, A. Fert, and W. Zhao, Nat. Commun. **9**, 671 (2018).
[4] S. Peng, D. Zhu, J. Zhou, B. Zhang, A. Cao, M. Wang, W. Cai, K. Cao, and W. Zhao, Adv. Electron. Mater. **5**, 1900134 (2019).
[5] Y. Liu and Z. Zhang, Sci. China Phys. Mech. Astron. **56**, 184 (2013).
[6] J. C. Slonczewski, J. Magn. Magn. Mater. **159**, L1 (1996).
[7] J. C. Slonczewski, Phys. Rev. B **39**, 6995 (1989).
[8] L. Berger, Phys. Rev. B **54**, 9353 (1996).
[9] I. M. Miron, G. Gaudin, S. Auffret, B. Rodmacq, A. Schuhl, S. Pizzini, J. Vogel, and P. Gambardella, Nat. Mater. **9**, 230 (2010).
[10] I. M. Miron, K. Garello, G. Gaudin, P. J. Zermatten, M. V. Costache, S. Auffret, S. Bandiera, B. Rodmacq, A. Schuhl, and P. Gambardella, Nature (London) **476**, 189 (2011).
[11] Y. Ou, S. Shi, D. C. Ralph, and R. A. Buhrman, Phys. Rev. B **93**, 220405(R) (2016).
[12] L. Liu, C. F. Pai, Y. Li, H. W. Tseng, D. C. Ralph, and R. A. Buhrman, Science **336**, 555 (2012).
[13] Y. W. Oh, S. H. C. Baek, Y. M. Kim, H. Y. Lee, K. D. Lee, C. G. Yang, E. S. Park, K.S . Lee, K. W. Kim, G. Go, J. R. Jeong, B. C. Min, H. W. Lee, K. J. Lee, and B. G. Park, Nat. Nanotechnol. **11**, 878 (2016).
[14] M. Ali, C. H. Marrows, M. Al-Jawad, B. J. Hickey, A. Misra, U. Nowak, and K. D. Usadel, Phys. Rev. B. **68**, 214420 (2003).
[15] S. Peng, D. Zhu, W. Li, H. Wu, A. J. Grutter, D. A. Gilbert, J. Lu, D. Xiong, W. Cai, P. Shafer, K. L. Wang, and W. Zhao, Nat. Electron. **3**, 757 (2020).
[16] G. Vermijs, A. Solignac, J. Koo, J. T. Kohlhepp, H. J. M. Swagten, B. Koopmans, and A. Van Den Brink, Nat. Commun. **7**, 10854 (2016).
[17] Y. C. Lau, D. Betto, K. Rode, J. M. D. Coey, and P. Stamenov, Nat. Nanotechnol. **11**, 758 (2016).
[18] S. Fukami, C. Zhang, S. Duttagupta, A. Kurenkov, and H. Ohno, Nat. Mater. **15**, 535 (2016).

[19] Y. Liu, B. Zhou, and J. G. (Jimmy) Zhu, Sci. Rep. **9**, 325 (2019).
[20] L. Chen, M. Gmitra, M. Vogel, R. Islinger, M. Kronseder, D. Schuh, D. Bougeard, J. Fabian, D. Weiss, and C. H. Back, Nat. Electron. **1**, 350 (2018).
[21] R. H. Liu, W. L. Lim, and S. Urazhdin, Phys. Rev. B **89**, 220409(R) (2014).
[22] Q. Huang, Y. Dong, X. Zhao, J. Wang, Y. Chen, L. Bai, Y. Dai, Y. Dai, S. Yan, and Y. Tian, Adv. Electron. Mater. **6**, 1900782 (2020).
[23] S. Kwon, P. V. Ong, Q. Sun, F. Mahfouzi, X. Li, K. L. Wang, Y. Kato, H. Yoda, P. K. Amiri, and N. Kioussis, Phys. Rev. B **99**, 064434 (2019).
[24] H. Lee, F. Ebrahimi, P. K. Amiri, and K. L. Wang, IEEE Magn. Lett. **7**, 3102505 (2016).
[25] H. Lee, A. Lee, F. Ebrahimi, P. Khalili Amiri, and K. L. Wang, IEEE Electron Device Lett. **38**, 1343 (2017).
[26] W. Kang, Y. Ran, W. Lv, Y. Zhang, and W. Zhao, IEEE Magn. Lett. **7**, 387 (2016).
[27] W. Kang, Y. Ran, Y. Zhang, W. Lv, and W. Zhao, IEEE Trans. Nanotechnol. **16**, 387 (2017).
[28] S. Z. Peng, J. Q. Lu, W. X. Li, L. Z. Wang, H. Zhang, X. Li, K. L. Wang, and W. S. Zhao, in *Proceedings of the 2019 IEEE International Electron Devices Meeting* (San Francisco, CA, USA, 2019), p. 28.6.1.
[29] S. Peng, S. Li, W. Kang, J. Zhou, N. Lei, Y. Zhang, H. Yang, X. Li, P. K. Amiri, K. L. Wang, and W. Zhao, Appl. Phys. Lett. **111**, 152403 (2017).
[30] M. Tsujikawa and T. Oda, Phys. Rev. Lett. **102**, 247203 (2009).
[31] H. Yoda, N. Shimomura, Y. Ohsawa, S. Shirotori, Y. Kato, T. Inokuchi, Y. Kamiguchi, B. Altansargai, Y. Saito, K. Koi, H. Sugiyama, S. Oikawa, M. Shimizu, M. Ishikawa, K. Ikegami, A. Kurobe, and A. H. Density, in *Proceedings of the IEEE International Electron Devices Meeting* (San Francisco, CA, USA, 2016), p. 27.6.1.
[32] T. Inokuchi, H. Yoda, Y. Kato, M. Shimizu, S. Shirotori, N. Shimomura, K. Koi, Y. Kamiguchi, H. Sugiyama, S. Oikawa, K. Ikegami, M. Ishikawa, B. Altansargai, A. Tiwari, Y. Ohsawa, Y. Saito, and A. Kurobe, Appl. Phys. Lett. **110**, 252404 (2017).
[33] W. S. Zhao, Z. H. Wang, S. Z. Peng, L. Z. Wang, L. Chang, and Y. G. Zhang, Sci. Sin. Phys. Mech. Astron. **46**, 107306 (2016).
[34] D. Wu, G. Yu, C. T. Chen, S. A. Razavi, Q. Shao, X. Li, B. Zhao, K. L. Wong, C. He, Z. Zhang, P. Khalili Amiri, and K. L. Wang, Appl. Phys. Lett. **109**, 222401 (2016).
[35] See Supplemental Material at http://link.aps.org/supplemental/10.1103/PhysRevB.103.094436 for further information on the impact of leakage current, the quantitative discussion about the reduction of critical current, critical current dependence of anisotropy energy, and further information on voltage dependence of saturation magnetization.
[36] M. Hayashi, J. Kim, M. Yamanouchi, and H. Ohno, Phys. Rev. B. **89**, 144425 (2014).
[37] X. Qiu, P. Deorani, K. Narayanapillai, K. S. Lee, K. J. Lee, H. W. Lee, and H. Yang, Sci. Rep. **4**, 4491 (2014).
[38] X. Li, G. Yu, H. Wu, P. V. Ong, K. Wong, Q. Hu, F. Ebrahimi, P. Upadhyaya, M. Akyol, N. Kioussis, X. Han, P. Khalili Amiri, and K. L. Wang, Appl. Phys. Lett. **107**, 142403 (2015).
[39] K. S. Lee, S. W. Lee, B. C. Min, and K. J. Lee, Appl. Phys. Lett. **102**, 112410 (2013).